Impact Modification of Polyamid 11

M. MEHRABZADEH[1,*] and R. P. BURFORD[2]

[1]Polymer Research Center of Iran, P.O. Box 14185/458, Tehran, Iran; [2]Department of Polymer Science, University of New South Wales, P.O. Box 1, Kensington, NSW, Australia 2033

SYNOPSIS

The results of this article are accepted as a provisional patent by a unisearch limited of the University of New South Wales in Australia in 1994. The low-impact behavior of polyamide 11 when modified by a butadiene–acrylonitrile copolymer ("nitrile rubber") was studied. The effect of the level of rubber addition and the acrylonitrile content is described. The rubber particle size and particle-size distribution were found to be important factors in controlling blend properties, including impact strength. SEM studies showed that toughness can be predicted by morphology. The mechanism of energy dissipation at low concentrations of rubber (≥20%) is crazing, plastic deformation, voiding, and matrix shear yielding. On the basis of these studies, it can be concluded that toughening of polyamide 11 is possible with nitrile rubber and that these blends are industrially compatible. © 1996 John Wiley & Sons, Inc.

INTRODUCTION

Polymer blending is widely used for toughening of thermoplastic elastomers and has assumed greater industrial and scientific importance over the past two decades.[1-4] Most of the widely used thermoplastic materials, such as isotactic polypropolyene (PP), polystyrene (PS), poly(vinyl chloride) (PVC), and polyamide (PA), show marked limitation in their end use because of poor impact resistance and toughness, particularly below their glass transition temperature. These limitations may be overcome to a certain extent by adding to the thermoplastic lower T_g rubbery components, by melt mixing, copolymerization, or other techniques.

The rubber particles dispersed in the rigid matrix stop craze growth, which can lead to the formation and development of failure cracks during impact, and at the same time, the particles act as stress concentrators, forming a barrier to the extension of crazing. The important factors in rubber toughening are "rubber concentration" and "rubber particle size," since these parameters fix the "interparticle distance," which is a very important factor in rubber toughening as it determines the stress state in front of the crack tip.

Generally, crazing, shearbanding, and cavitation occur prior to impact fracture and theories which explain micromechanisms of toughening include the role of rubber particles as stress concentrators and craze arresters.[5-12] Initially, rubber particles were taught to bridge cracks[13] and this "microcrack" theory was extended by the multiple crazing theory of Buknall and Smith,[14] where rubber particles both initiate and control craze growth. Newman and Strella[15,16] postulated enhancement of matrix shear yielding, while cavitation has also been proposed.[17,18]

Rubber cavitation under triaxial tension arises from elastic instability of "precavities," and so voiding in the blend is predicted to depend entirely upon the rubber modulus. Further refinements of rubber cavitation/matrix plastic deformation theories have also appeared.[19,20]

One group of thermoplastic elastomers of particular interest are the polyamides. Dry polyamides are semiductile materials at room temperature. Above their T_g, they are tough and exhibit reasonably high tensile strength and elongation to break. Polyamides have high impact strength but are notch-sensitive. They have good resistance to crack initiation, but poor resistance to crack propagation.

* To whom correspondence should be addressed.

Journal of Applied Polymer Science, Vol. 61, 2305–2314 (1996)
 CCC 0021-8995/96/132305-10

Table I Mechanical and Oil Swelling Properties of PA11/NBR(LAN) : 80/20 Blends, ABS, and HIPS

Sample	Impact Strength (J/m)	Elongation at Break (%)	Tensile Strength (MPa)	Hardness D Scale	Oil Swell, Increase (%) 70 h, 125°C, ASTM Oil No. 3		
					In Weight	In Thickness	In Width
PA11	25	300	50	72	1.30	0.25	0.2
I	55	52	21	61	3.56	1.55	0.31
II	100	116	25	60	1.59	0.25	0.15
III	1840	132	27	60	1.05	0.20	0.10
ABS	333	26	43	78	19.32	30.90	9.16
HIPS	92	11	28	75	101.30	The shape is changed	

There are three ways to improve the impact strength of polyamide: (a) plasticizing with water, (b) addition of a copolymer (block copolymerization) as a soft segment, and (c) the incorporation of a dispersed rubber phase by reaction blending. Polyamides are usually toughened by incorporation of rubber or of elastomers as impact modifiers such as hydrocarbon rubber,[21,22] acrylic rubber,[23] ethylene–ethyl acrylate,[24] SEBS, and SEBS-*g*-MA (Refs. 25 and 26) EPR, and mostly with EPDM and EPDM-*g*-MA.[27,29] Generally, the polyamides used are based on PA6 and PA6,6 which are important commercial polyamides. Although it is possible to toughen polyamides as described above, it has not been possible to produce polyamides that are comparable with tough engineering plastics such as high-impact polystyrene (HIPS) and acrylonitrile–butadiene–styrene (ABS).

EXPERIMENTAL

The thermoplastic used throughout was a natural grade of polyamide 11, Rilsan, BMW. This has a fine particle size and is white and of an unmodified injection-molding grade provided by Atochem, France. The butadiene–acrylonitrile (nitile) elastomer employed was krynac 19.65 (19% AN), provided by Polysar, Canada.

Blend Preparation

Blends were prepared by a melt-mixing technique, and to explain the effect of the processing technique and particle size on the mechanical properties in a low rubber content PA11/NBR (L.AN), 80/20 blends, three samples are made as follows: Sample I: Pelletized NBR is completely physically mixed with dried polyamid 11 powder and the mixture is

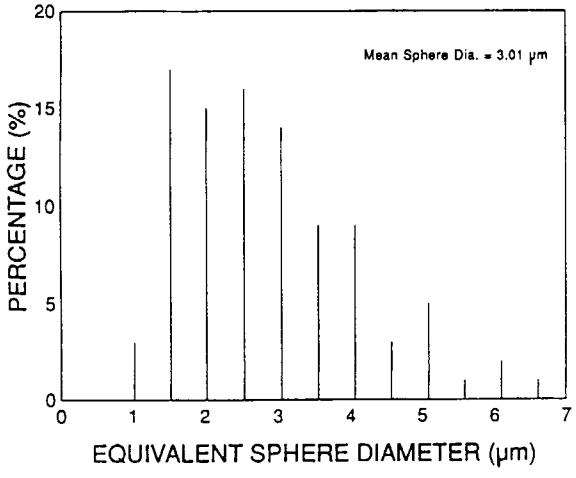

Figure 1 Rubber particle size and particle-size distribution of PA11/NBR(L.AN) : 80/20 blends, sample I.

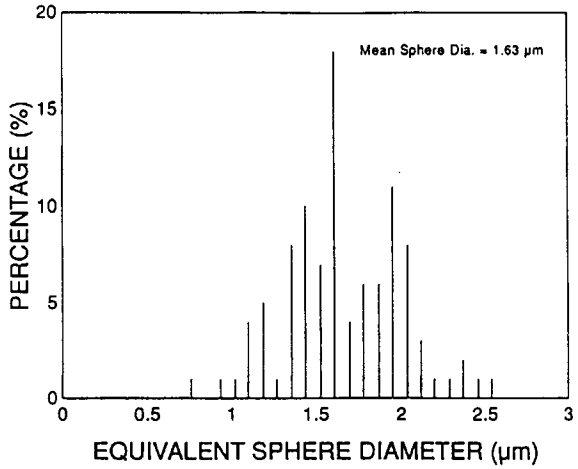

Figure 2 Rubber particle size and particle-size distribution of PA11/NBR(L.AN) : 80/20 blends, sample II.

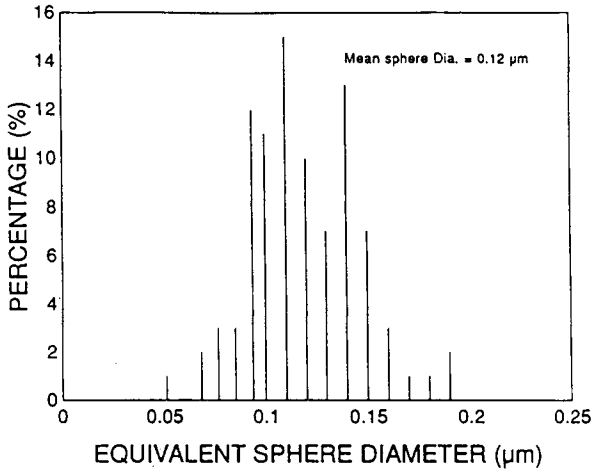

Figure 3 Rubber particle size and particle-size distribution of PA11/NBR(L.AN) : 80/20 blends, sample III.

used in a Johns CF 550 injection-molding machine. Samples II and III: Pelletized NBR is completely physically mixed with dried polyamid 11 powder and the mixture is then put into a Bradender DSK twin-screw extruder. Then, the pletized extrudate is used in the injection-molding machine. The difference between samples II and III is additional mixing and shearing to reduce the particle size. Samples I, II, and III have a 3.01, 1.63, and 0.12 μm mean particle size, respectively. In each procedure, polyamide 11 powder was dried to remove moisture for 18 h at 60°C and the rubber was pelletized using a Crompton Parkinson granulator before use.

Mechanical Characterization

The injection-molding procedure employed a four-cavity mold, two cavities providing suitable samples for routine tensile and impact testing. At least three and typically five replicate samples were tested for both tensile and impact data. Tensile bars conformed to ASTM D-638, Type II, and were strained using a cross-head speed of 50 mm min^{-1} in an Instron 1115 universal testing machine.

Impact bars 60 × 12 × 6 mm (thin bars) and 55 × 14 × 10 mm (thick bars) were sharp-notched (2.5 mm) using a razor blade rather than employing the 45° notch specified in ASTM D-256. Impact testing was performed in Zwick 5102 pendulum machine (for thin bars) and a Satec System Model SI-ID3 pendulum machine with a 33.9 Joules head (for thick bars).

The rubber particle size and particle-size distribution of the blends are measured by an image analyzer (Optomax System) from SEM micrographs

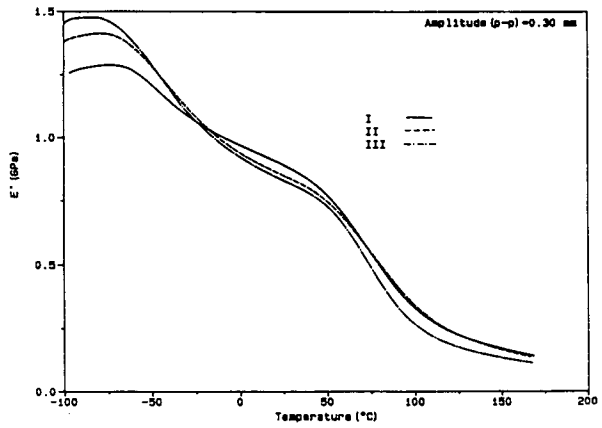

Figure 4 Storage modulus traces of PA11/NBR(L.AN) : 80/20 blends, with different processing.

of the fracture surface. Solvent resistance was measured by immersing 20 × 20 × 4 mm pieces of each blend in ASTM oil #3 for 70 h at 125°C, in accordance with ASTM D-471. Changes in weight and dimensions were recorded.

Thermal Behavior

Dynamic mechanical properties of the blends were performed using 23 × 10 × 4 mm injection-molded test pieces by using a DuPont 983 DMA and Series 2100 analyzer. The DMA system possessed liquid nitrogen cooling facilities (LNCA II) which allowed testing to be completed over the temperature range of −100 to 180°C at 20°C/min.

RESULTS AND DISCUSSION

In a previous article,[30] we explained the effect of rubber content and acrylonitrile content and we

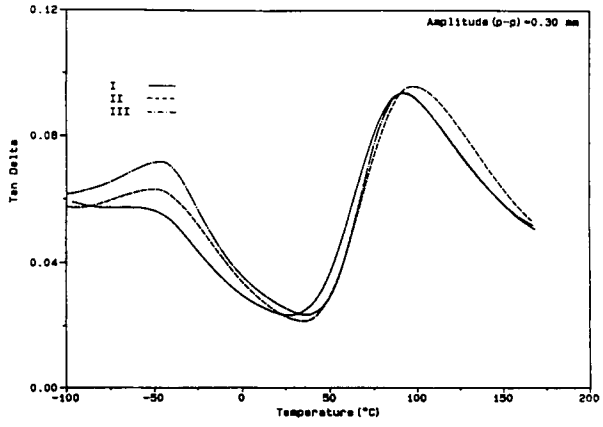

Figure 5 Tan δ traces of PA11/NBR(L.AN) : 80/20 blends, with different processing.

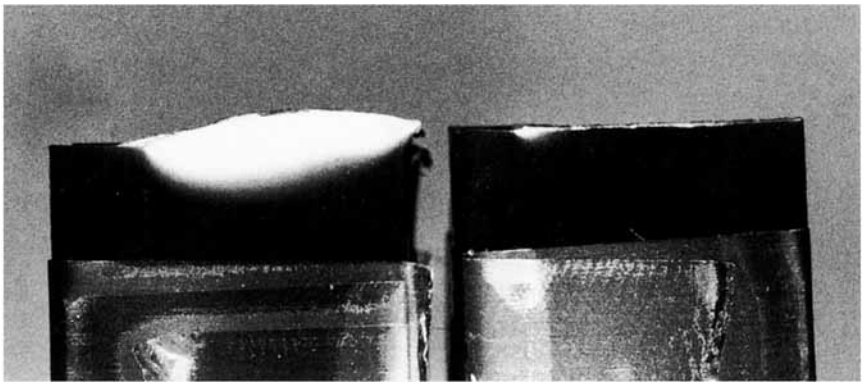

Figure 6 Optical micrograph of stress-whitened zone of PA11/NBR(L.AN) : 80/20 blends, from left to right: samples III and II.

concluded that by increasing the rubber content and decreasing the %AN content the impact strength increase. In the present article, the effect of particle size and processing conditions on impact modification are described. The results of these studies are accepted as a provisional patent in Australia.

To improve further the impact strength for low rubber content blends, we decided to reduce the rubber particle size and to optimize mixing conditions. For this to be achieved, there are several techniques including changing shear rate, temperature, etc. We used a twin-screw extruder to achieve a smaller particle size and better particle-size distribution (better mixing).

Table I shows the mechanical and oil swelling properties of PA11/NBR(L.AN) : 80/20 blends which are made with different procedures and different particle sizes. For comparing our results with other tough engineering plastics, we chose high-impact polystyrene (HIPS) and the high-impact acrylonitrile–butadiene–styrene copolymer (ABS), which are commercial tough engineering plastics. The same conditions were applied for testing the ABS and HIPS and the results are also shown in Table I.

It can be seen from Table I that by changing the processes the impact strength increases with sample III having a very high impact strength "supper-tough." The elongation at break and oil swelling resistance are also improved. Comparing the results of sample III with ABS and HIPS, PA11/NBR (L.AN) : 80/20 blends constitute both a supertough polyamide 11 and a good engineering plastic.

Figures 1–3 show the rubber particle size and particle-size distribution of sample I–III, respectively. It can be seen that by changing the processing history the rubber particle diameter decreased, from 3.01 μm in sample I (Fig. 1), to 1.63 μm in sample II, and to 0.12 μm in sample III. We conclude that the improvement in mechanical properties of the

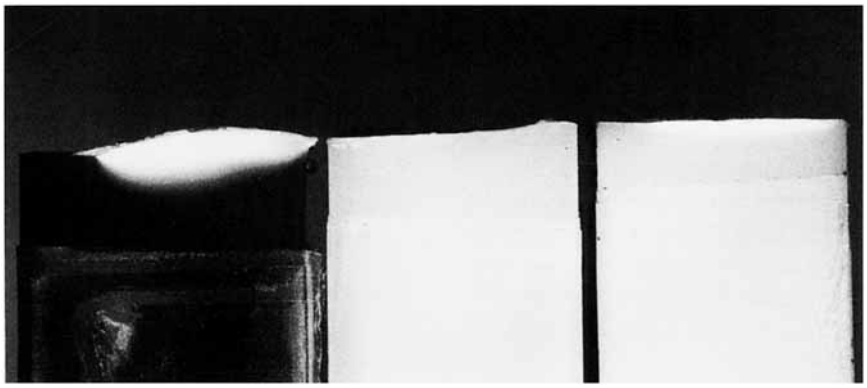

Figure 7 Optical micrograph of stress-whitened zone, from left to right: PA11/NBR(L.AN) : 80/20 blend, HIPS, and ABS.

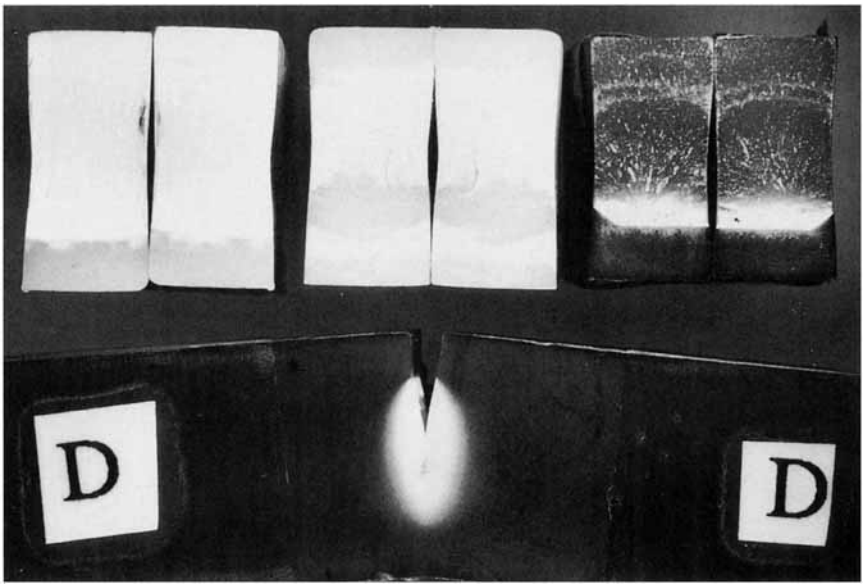

Figure 8 Optical micrograph of Charpy notched fracture surface of (top from left to right, respectively) ABS, HIPS, and sample II and (bottom) sample III ("supertough" polyamide 11).

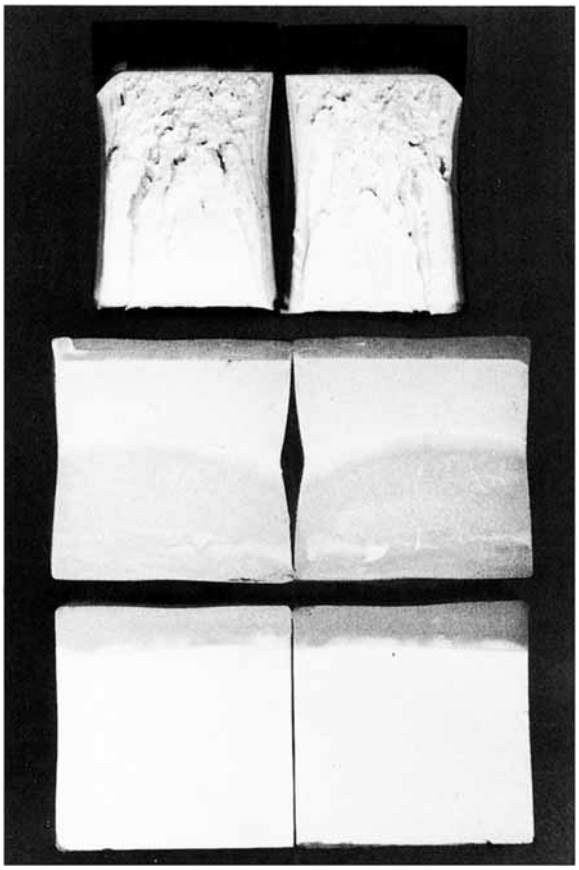

Figure 9 Stress-whitened zones of Charpy notched impact fracture surface of (top) sample III, (middle) HIPS, and (bottom) ABS.

sample III is due to small particle size and better particle-size distribution.

Thermal Behavior

DMA and DSC show that by changing the process partial miscibility is increased. Figures 4 and 5 show the storage modulus and tan δ of PA11/NBR(L.AN) : 80/20 blends with different processing techniques (corresponding to samples I–III in Table I). It can be seen that (Fig. 4) by decreasing the particle size the storage modulus decreases, which is correlated with impact improvement. Tan δ (Fig. 5) traces show a slight increase in the T_g of NBR, which is related to improvement of partial miscibility.

Morphological Observation

The notched Charpy fracture surface of samples I–III at low rubber content were studied optically and by using SEM. High toughness values are consistent with the fracture morphology, with the toughened polyamide (sample III) being grossly whitened and plastically deformed at and below the fracture surface. This is seen to be more extensive than that for the other polyamide samples (different processing) and the HIPS and ABS polymers (Figs. 6 and 7).

Figure 6 shows the stress-whitened zones for samples II and III. It can be seen that by decreas-

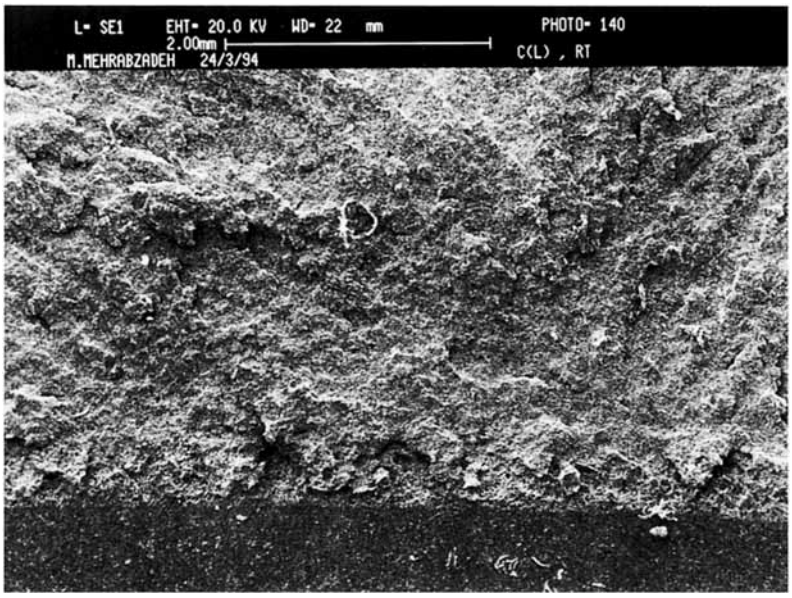

Figure 10 SEM micrograph of Charpy impact fracture surface of PA11/NBR(L.AN) : 80/20, sample II, at notch tip.

ing the particle size (sample III, left) which is supertough, the stress-whitened zone continued up to end of the fracture surface and high plastic deformation; for sample I, no stress-whitened zone was observed. Figure 7 shows the stress-whitened zones for the tough polyamide 11 (left), HIPS (middle), and ABS (right). This figure clearly shows for HIPS that there is little plastic deformation below the fracture surface, while for ABS, there is some. However, for the tough polyamide 11, the stress-whitened zone is much greater, indicating that it is very tough.

Figure 8 shows a Charpy notched fracture surface and a surface stress-whitened zone of thin samples (thickness 6 mm), to which the heaviest pendulum head (4 Joules) of a Zwick 5102 pendulum machine was applied. The figure shows that for the supertough polyamide 11 (sample III, bottom) the rupture

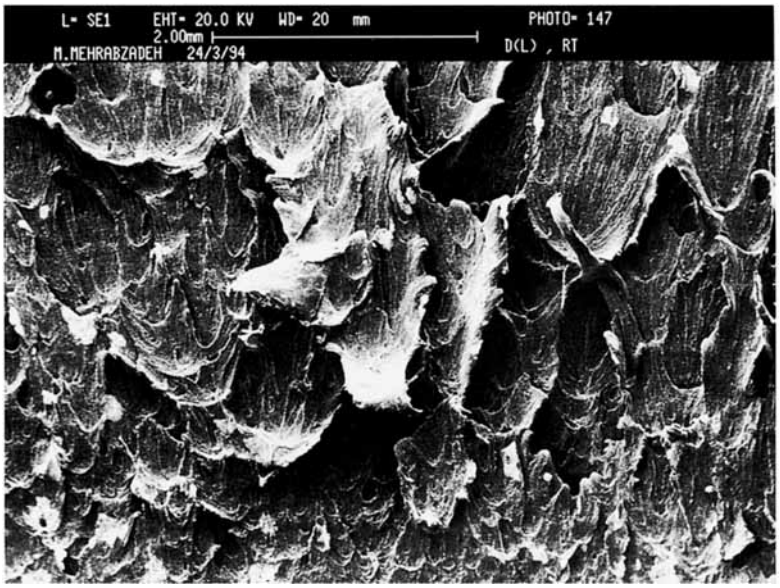

Figure 11 SEM micrograph of Charpy impact fracture surface of PA11/NBR(L.AN) : 80/20, sample III, at notch tip.

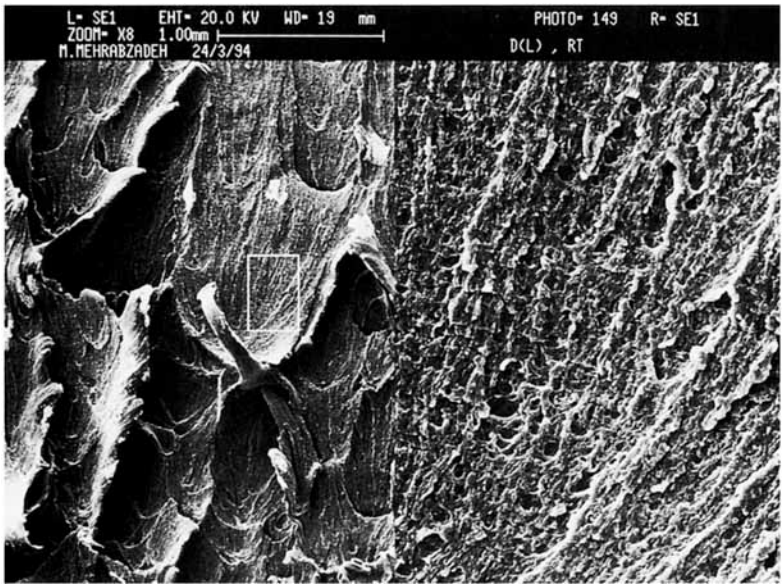

Figure 12 SEM micrograph of Charpy impact fracture surface of P11/NBR(L.AN) : 80/20, sample III.

was incomplete, but that for sample II, the HIPS and ABS controls were broken.

Figure 9 shows the Charpy notched fracture surface of large samples (thickness 10 mm) tested with a Statec System, SI-ID3 pendulum machine, with a maximum load head of 33.9 Joules. It can be seen that the stress-whitened zone for the supertough polyamide 11 (top) and ABS (bottom) continues from the notch tip toward the end of the fracture, but for HIPS (middle), about half of fracture surface is whitened. The tough PA11 fracture surface indicates greater toughness than for the ABS or HIPS, which have a smooth fracture surface.

The Charpy notched fracture surfaces of the samples at room temperature and low temperature were studied by SEM. Figures 10 and 11 show the fracture surface of samples II and III at the notch tip at the same magnification. It can be seen that

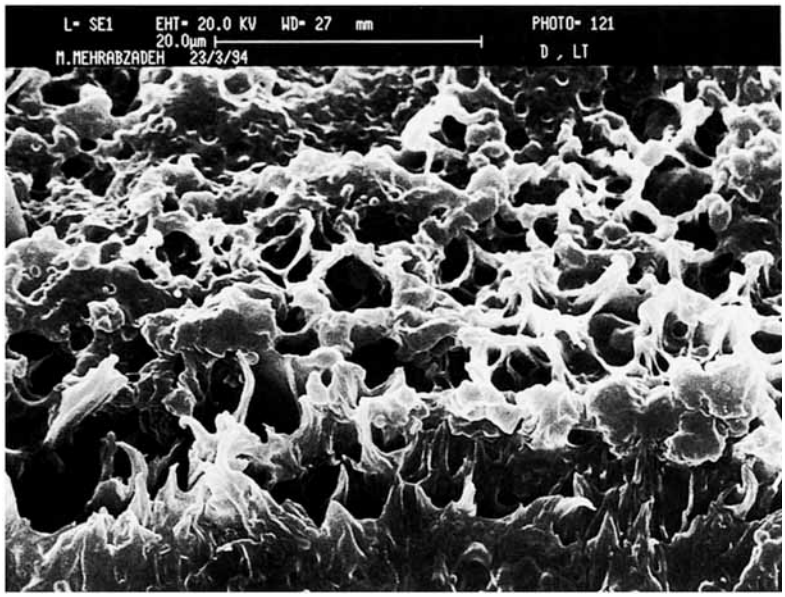

Figure 13 SEM micrograph of Charpy impact fracture surface of PA11/NBR(L.AN) : 80/20, sample III, at low temperature, at notch tip.

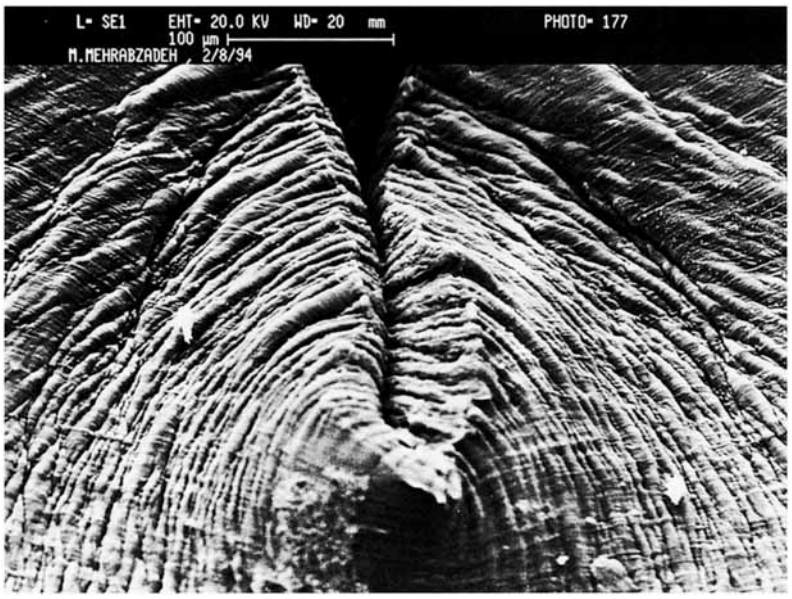

Figure 14 SEM micrograph of Charpy impact of PA11/NBR(L.AN) : 80/20, sample III, at the end of the notch.

sample III had a very tough fracture surface compared with sample II. Figure 12 also shows the plastic deformation, shear bands, and matrix drawing of the tough fracture surface of sample III.

At high magnification, both samples II and III show cavitation and matrix drawing at the notch tip. The cavitation and matrix drawing are much more extensive for sample III and continues up to end of the fracture surface. For sample III, even at low temperatures (below 0°C), cavitation and matrix drawing were observed at the notch tip (Fig. 13). Figures 14 and 15 show the crazing and shear bands which occur in supertough polyamide 11 (sample III).

On the basis of optical and SEM micrographs, the mechanism of energy dissipation in "supertough polyamide 11" is multiple crazing due to small rubber particles and shear bands due to matrix plastic de-

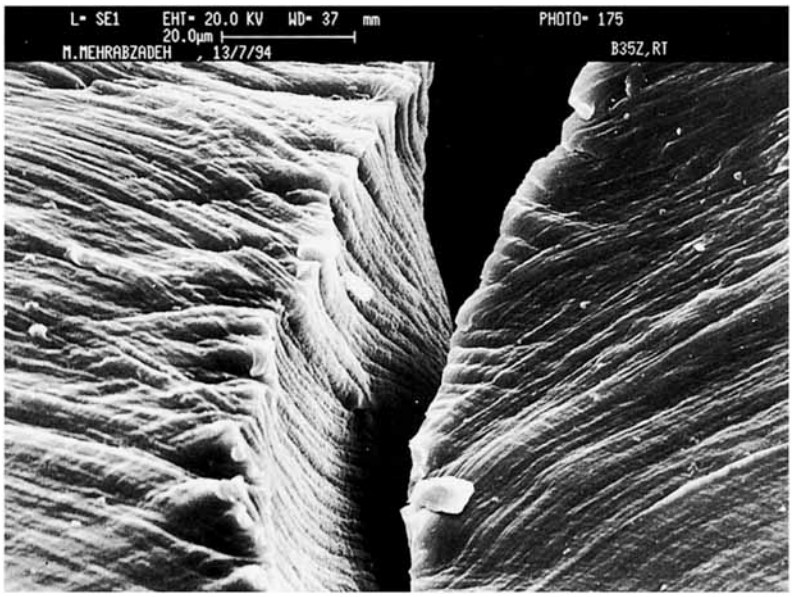

Figure 15 SEM micrograph of charpy impact of PA11/NBR(L.AN) : 80/20, sample III; shear bands are observed in micropraph.

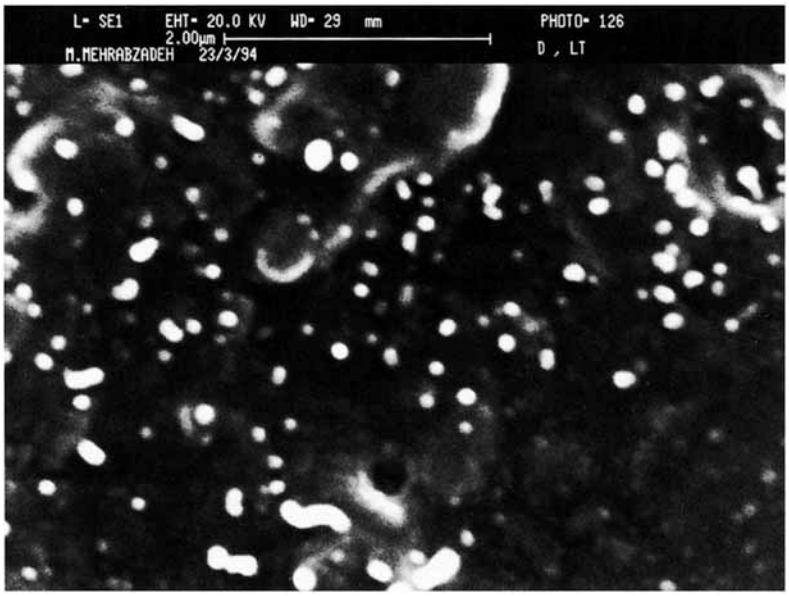

Figure 16 SEM micrograph of rubber particles in Charpy fracture surface of PA11/NBR(L.AN) : 80/20, sample III, at low temperature, stained with OsO4.

formation. On the other hand, rubber particles relieve the hydrostatic tension ahead of the crack tip, by creating voids.

We observed the rubber particles further away from notch tip for samples II and III in low-temperature fracture surfaces. Figure 16 shows rubber particles for sample III at high magnification (×20,000).

CONCLUSION

On the basis of these studies, it can be concluded that by changing the processing history and decreasing the rubber particle size we can make "supertough" polyamide 11 with NBR. By decreasing the particle size in PA11/NBR : 80/20 blends, the stress-whitened zone increases, and at a particle size about 0.12 μm, the stress-whitened zone continued to the end of the fracture surface and below the fracture surface, with high plastic deformation.

SEM and optical studies showed that the major mechanism of energy dissipation in "supertough polyamide 11" is multiple crazing due to small rubber particles and shear bands associated with matrix plastic deformation. Voiding and cavitation are also two forms of energy dissipation. Some energy may also dissipate by stretching, deformation, and tearing of rubber particles and matrix shear yielding.

REFERENCES

1. L. A. Utracki, *Polymer Alloys and Blends,* Hanser, New York, 1989.
2. D. R. Paul and R. Newsman, *Polymer Blends,* Academic Press, New York, 1978, Vols. 1 and 2.
3. J. T. Lutz, *Thermoplastic Polymer Additives,* Marcel Dekker, New York, 1989.
4. K. Solc, *Polymer Compatibility and Incompatibility: Principles and Practice,* Vols. 1 and 2, MMI Press Symposium Series, Harwood, New York, 1986.
5. R. J. M. Borggreve, R. J. Gaymans, and N. M. Eichenwald, *Polymer,* **30,** 78 (1980).
6. S. Kunz, P. W. Beaumont, and M. F. Ashby, *Mater. Sci.,* **15,** 1109 (1980).
7. A. F. Yee and R. A. Pearson, *Mater. Sci.,* **21,** 2462 (1986).
8. R. J. M. Borggreve, R. J. Garmans, and J. Schuiser, *Polymer,* **30,** 71 (1989).
9. F. Speroni and E. Castolli, *Mater. Sci.,* **24,** 2165 (1989).
10. R. J. Gaymans, R. J. M. Borggreve, and A. J. Oostenbrink, *Makromol. Chem. Macromol. Symp.,* **38,** 125 (1990).
11. D. F. Lawson, W. L. Hergenruther, and M. G. Mattock, *J. Appl. Polym. Sci.,* **39,** 2331 (1990).
12. E. H. Merz, G. C. Claver, and M. Baer, *J. Polym. Sci.,* **22,** 325 (1956).
13. C. B. Buknall, *Rubber Toughened Plastic,* Applied Science, London, 1977, Chap. 7.
14. C. B. Buknall and R. R. Smith, *Polymer,* **6,** 437 (1955).

15. S. Newman and S. Strella, *J. Appl. Polym. Sci.*, **9,** 2297 (1965).
16. S. Strella, *J. Polym. Sci. A-2,* **3,** 527 (1966).
17. A. N. Gent, in *Science and Technology of Rubber,* F. R. Eirich, Ed., Academic Press, New York, 1978, Chap. 10.
18. A. N. Gent and D. A. Tompkins, *J. Polym. Sci. A2,* **7,** 1483 (1969).
19. F. Ramsteiner, *Kustoffe,* **73,** 148 (1983).
20. F. Ramsteiner and W. Hecmann, *Polym. Commun.,* **26,** 199 (1985).
21. S. Wu, *J. Polym. Sci. Polym. Phys.,* **21,** 699 (1983).
22. S. Wu, *Polymer,* **26,** 1855 (1985).
23. J. D. Katsaros and D. G. Grimes, *Plast. Eng.,* **Aug.** (1990).
24. D. M. Kung and G. H. Williams, *Plast. Eng.,* Apr. (1990).
25. M. J. Modic and L. A. Pottick, *Plast. Eng.,* **37** (1991).
26. A. J. Oshinski, H. Keskkula, and D. R. Paul, in *Proceedings of the American Chemical Society, Division of Polymeric Materials,* Spring Meeting, Georgia, 1991.
27. P. J. Lemstra and L. A. Kleintjens, *Integration of Fundamental Polymer Science and Technology,* Elsevier, London, 1988, Vol. 2.
28. S. Wu, *Polym. Eng. Sci.,* **27,** 335 (1987).
29. S. Cimmino, L. D'orazio, R. Greco, G. Maglio, M. Malinconico, C. Mancarella, E. Martuscelli, R. Palumbo, and G. Ragosta, *Polym. Eng. Sci.,* **24,** 48 (1984).
30. M. Mehrabzadeh and R. P. Burford, *Iran. J. Polym. Sci. Technol.,* **14**(3), 156 (1995).

Received November 21, 1995
Accepted March 30, 1996